

Fast reactive flow simulations using analytical Jacobian and dynamic load balancing in OpenFOAM

Ilya Morev^{*a}, Bulut Tekgöl^a, Mahmoud Gadalla^a, Ali Shahanaghi^a,
Jeevananthan Kannan^a, Shervin Karimkashi^a, Ossi Kaario^a, Ville Vuorinen^a

^a*Department of Mechanical Engineering, Aalto University School of Engineering,
Otakaari 4, 02150 Espoo, Finland.*

Abstract

Detailed chemistry-based computational fluid dynamics (CFD) simulations are computationally expensive due to the solution of the underlying chemical kinetics system of ordinary differential equations (ODEs). Here, we introduce a novel open-source library aiming at speeding up such reactive flow simulations using OpenFOAM, an open-source software for CFD. First, our dynamic load balancing model by Tekgöl et al. [DLBFoam: An open-source dynamic load balancing model for fast reacting flow simulations in OpenFOAM, *Computer Physics Communications* 267 (2021)] is utilized to mitigate the computational imbalance due to chemistry solution in multiprocessor reactive flow simulations. Then, the individual (cell-based) chemistry solutions are optimized by implementing an analytical Jacobian formulation using the open-source library pyJac, and by increasing the efficiency of the ODE solvers by utilizing the standard linear algebra package (LAPACK). We demonstrate the speed-up capabilities of this new library on various combustion problems. These test problems include a 2-dimensional (2D) turbulent

^{*}Corresponding Author. E-mail address: ilya.morev@aalto.fi

reacting shear layer and 3-dimensional (3D) stratified combustion to highlight the favourable scaling aspects of the library on ignition and flame front initiation setups for dual-fuel combustion. Furthermore, two fundamental 3D demonstrations are provided on non-premixed and partially premixed flames, namely the Engine Combustion Network Spray A and the Sandia flame D experimental configurations, which were previously considered unfeasible using OpenFOAM. The novel model offers up to two orders of magnitude speed-up for most of the investigated cases. The openly shared code along with the test case setups represent a radically new enabler for reactive flow simulations in the OpenFOAM framework.

Keywords: Reacting flow, Chemical kinetics, OpenFOAM, Dynamic load balancing, Jacobian

1. Introduction

There is an urgent need to develop effective and accurate engineering solutions to combat climate change. Reactive flow simulations play an essential role in academic and industrial research on mitigating harmful emissions. A number of computational fluid dynamics (CFD) packages are available on the market, offering a variety of features together with possible limitations. Major limitations related to software distribution under commercial licenses are their affordability and source code access. The imminent pace of climate change urges us to broaden the use of the latest achievements in CFD beyond the limitations of commercial software to all appropriate applications. Unfortunately, the available open-source reacting flow solvers are currently limited. The most popular open-source general-purpose CFD code – OpenFOAM –

poses relatively poor performance for finite rate chemistry simulations compared to commercial solutions, making it impractical for large-scale industrial applications and thus limiting its use to relatively simple academic cases. However, the importance of open-source solutions was recently recognized at a governmental level. For instance, there is a large ongoing project funded by the European Union on optimizing the OpenFOAM code – exaFoam [1]. In this work, we proceed in a similar track and focus on the search for the bottlenecks in reacting flow simulations within OpenFOAM with the aim of significant computational speed-up.

One of the most fundamental approaches for reactive flow modeling is to use CFD with the direct integration of chemical kinetics, referred to as finite-rate chemistry [2]. In this approach, each computational cell is treated as an individual chemistry problem with pressure (p), and a thermochemical state vector (Φ) comprising temperature (T) and species mass fractions (Y_k). The rate of change of the thermochemical state vector, $\partial\Phi/\partial t = \mathbf{f}(\Phi, t)$, within a computational cell forms stiff system of ordinary differential equations (ODEs) that requires a specific class of algorithms for temporal integration.

In reactive CFD applications, chemistry evaluation comprises the most computationally demanding part of the simulation. With the growing complexity of chemical kinetic mechanisms, the cost of solving the chemistry problem often exceeds the cost of fluid flow solution by up to two orders of magnitude [3]. Nevertheless, high-fidelity reactive flow simulations can be still feasible through efficient usage of the provided computational resources, in addition to cell-based optimization of the chemistry solution [4]. In gen-

eral, considerable efforts have been made in the literature to improve the computational performance of CFD simulations involving turbulence [5–9], shock waves [10], gas rarefaction [11], geometrical parameterization [12], or chemical reactions [13–16] through model reduction, machine learning, or efficient parallelization.

In finite-rate chemistry simulations, the high computational cost associated with the chemistry solution originates mainly from two factors. First, the cost of solving the system of ODEs depends on the system stiffness which is, to some extent, influenced by the local thermochemical state. For example, an oxidation process comprising different radicals at various chemical timescales may constitute a greater computational challenge compared to a local state of burnt mixture. Second, the cost of computing the rate of change of the thermochemical state vector is directly proportional to the chemical mechanism size [17, 18], which can reach up to thousands of species and even more reactions [19, 20].

For the chemistry ODE problem, implicit solvers involving Jacobian evaluation are usually preferred over explicit ones for stability and accuracy reasons [21]. The evaluation of the Jacobian, $\mathcal{J} = \partial \mathbf{f} / \partial \Phi$, is a computationally demanding process within an ODE solution routine. ODE solvers often employ finite differencing methods for its evaluation, which may be an expensive operation depending on the chemical mechanism size. Lu et al. [17] reported that the computational cost of numerical evaluation of Jacobian scales quadratically with the number of reactions. It has been shown that using an analytically computed Jacobian provides high performance gain during the ODE system solution [17, 22, 23]. There are various implementations of

the analytical Jacobian matrix evaluation in the literature [23–25]. Recently, Niemeyer et al. [26] introduced an open-source library `pyJac`, which generates C subroutines for analytical Jacobian evaluation. They demonstrated its accuracy and out-performance over the available analytical Jacobian generators in the literature.

While the cost of integrating a single chemistry ODE problem poses a performance challenge in reactive CFD simulations, there is a secondary issue which is often left unaddressed. As previously mentioned, the computational cost of solving a chemistry ODE depends on the local stiffness of Φ . The difference in computational complexity throughout the geometrical domain poses a load imbalance issue for multiprocessor applications, where one process becomes the computational bottleneck and causes performance issues. There have been several studies in the recent literature tackling this load imbalance issue via utilizing dynamic load balancing algorithms, often using Message-Passing Interface (MPI) routines. Antonelli et al. [27] developed an MPI-based model introducing a cell distribution based load balancing algorithm. Following this work, Shi et al. [28] and Kodavasal et al. [29] both introduced stiffness-detection based load balancing algorithms and employed them in reactive CFD simulations. Zirwes et al. developed an MPI-based dynamic load balancing algorithm for chemistry problem distribution for OpenFOAM [30]. More recently, Muela et al. [31] presented a dynamic load balancing model, which also utilizes a stiffness detection algorithm that chooses the optimal ODE integration method for each computational cell. These methods introduced computational speed-up around 3 to 5, depending on the application. We have recently also introduced an

open-source dynamic load balancing model called DLBFoam for OpenFOAM, providing speed-up up to a factor of 10 [4].

In this work, we introduce a novel chemistry model that provides speed-up in reactive flow simulations in OpenFOAM by targeting the two major issues in reactive CFD simulations addressed above. We further extend our dynamic load balancing model DLBFoam, and focus on the optimization of the cell-wise chemistry solution by introducing two new features. First, we utilize an analytical Jacobian approach using the pyJac library. Second, we make use of the standard linear algebra library (LAPACK) [32] to further improve the ODE solution procedure of the chemistry problem, by replacing the LU decomposition and back substitution operations of the Seulex ODE integration algorithm in OpenFOAM with more robust alternatives suitable for dense Jacobian matrices. The effectiveness and robustness of the developed model are demonstrated on two different academic dual-fuel (DF) combustion set-ups: a 2-dimensional (2D) reacting shear layer and a 3-dimensional (3D) stratified combustion configuration. After that, the model is further demonstrated in two well-established experimental flame configurations: a non-premixed *n*-dodecane flame (Engine Combustion Network (ECN) Spray A), and a partially-premixed methane-air flame (Sandia flame D).

The paper is outlined as follows. First, implementation details of the developed model are presented in Section 2. Then, in Section 3 we discuss the application of our model to different combustion simulations, represented by the aforementioned test cases. Finally, conclusions are provided in Section 4.

2. Implementation

In this section, implementation details of our model are presented. We note that an earlier in-house version of this implementation was carried out by Kahila et al. [33], details of which can be found in his thesis work [34]. This section briefly discusses the `DLBFoam` model introduced by Tekgül et al. [4] as an improvement to our in-house code, and further describes the efforts towards optimizing the solution of the chemistry ODE problem by utilizing an analytical Jacobian formulation (`pyJac`) together with efficient linear algebraic routines (`LAPACK`).

2.1. Finite rate chemistry

In reactive CFD applications, we numerically solve the governing equations for mass, momentum, energy, and species transport. The total production or consumption rate of chemical species, and the heat release rate are represented as source terms in the species transport equations and the energy equation, respectively. Due to the vast difference between the chemistry and flow time scales, commonly an operator splitting procedure is utilized to separate the calculation of source terms from the flow solution. These source terms define the change of the local thermochemical state which results from solving a stiff, nonlinear initial value problem described as:

$$\begin{cases} \partial\Phi/\partial t = \left\{ \frac{\partial T}{\partial t}, \frac{\partial Y_1}{\partial t}, \frac{\partial Y_2}{\partial t}, \dots, \frac{\partial Y_{N_{sp}-1}}{\partial t} \right\}^T = \mathbf{f}(\Phi, t), \\ \Phi(t=0) = \Phi_0, \end{cases} \quad (1)$$

where N_{sp} is the number of species in the chemical mechanism. The ODE system in Equation (1) is integrated in each computational cell over the CFD

time step Δt_{CFD} in smaller chemical time steps $\Delta t_{\text{ODE}} \leq \Delta t_{\text{CFD}}$ (see Part C for more information). The source terms are then evaluated and used in species transport and energy equations. Further details on this modeling approach can be found in the work of Imren and Haworth [35].

2.2. Dynamic load balancing: DLBFoam

Next, the previously developed DLBFoam library is briefly introduced here as essential background information. As mentioned earlier, the computational cost of solving the stiff nonlinear ODE may depend on the local thermochemical conditions. In multiprocessor reactive CFD simulations, the process with the highest computational load may take longer to compute than the rest, hence creating a bottleneck within the given CFD time step.

Recently, we introduced an open-source model called DLBFoam [4] for OpenFOAM, aiming to mitigate this imbalance issue in multiprocessor reactive CFD simulations via dynamic load balancing. DLBFoam uses MPI routines to redistribute the chemistry computational load evenly between processes during the simulation. Figure 1 demonstrates the computational imbalance caused by the direct integration of chemistry, and how it is mitigated by DLBFoam. In addition, DLBFoam introduces a zonal reference cell mapping method, which further lowers the computational cost by mapping a chemistry solution from a reference cell instead of explicitly solving it for ambient regions with low reactivity. In total, we reported around a factor of 10 speed-up in 3D reactive CFD simulations, compared to the standard OpenFOAM chemistry model. Further implementation details on DLBFoam can be found in our previous publication describing it in detail [4].

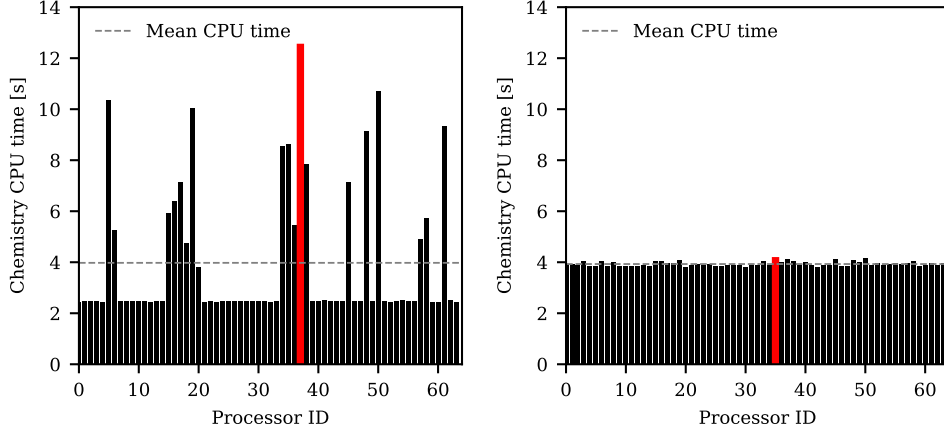


Figure 1: Left: The process-based computational imbalance in reactive CFD simulations without DLBFoam. The process with the highest computational load (red) creates a bottleneck in the simulation. Right: Same case with DLBFoam.

2.3. ODE solver optimization and analytical Jacobian

The new development in the present paper introduces a coupling of 1) the analytical Jacobian formulation introduced in pyJac library, 2) standard linear algebra routines from LAPACK library for the ODE solution, and 3) the DLBFoam library previously introduced by Tekgöl et al. [4]. Within a CFD time step, chemistry is treated as an independent, stiff system of ODEs. Implicit and semi-implicit algorithms for solving this system of stiff ODEs are usually preferred to ensure the solution stability [21].

The solution to the nonlinear initial value problem Equation (1), can be obtained using a variant of Newton iteration with the following discretized form

$$\begin{aligned}
 \Phi_{n+1} &= \Phi_n + \int_{t_n}^{t_n + \Delta t_{\text{ODE}}} (\mathbf{f}_n + \mathcal{J}_n(\Phi_{n+1} - \Phi_n) + \mathcal{O}(\Delta t_{\text{ODE}}^2)) dt \\
 &= \Phi_n + \mathbf{f}_n \Delta t_{\text{ODE}} + \mathcal{J}_n(\Phi_{n+1} - \Phi_n) \Delta t_{\text{ODE}} + \mathcal{O}(\Delta t_{\text{ODE}}^2),
 \end{aligned} \tag{2}$$

which is then linearized by neglecting the higher-order terms. Here, Δt_{ODE} is a subinterval of the full integration interval Δt_{CFD} , which is commonly determined by the underlying ODE solver using a combination of theoretical and heuristic relations. The direct solution of the previous equation for Φ_{n+1} requires the inverse of \mathcal{J} , which is commonly avoided through matrix factorization (i.e., LU decomposition) and back substitution techniques.

Commonly in reactive CFD codes, the Jacobian of the system of ODEs representing chemistry is implemented via finite differencing to be used in ODE solver integration. However, using such an approximation introduces a negative effect on the ODE solver accuracy and performance [26]. Furthermore, calculating the Jacobian with finite differencing is a computationally expensive procedure [17, 26]. Instead, utilizing a fully algebraic Jacobian is more efficient and it improves the ODE solver accuracy and performance. Lu et al. [17] reported that using an analytical Jacobian reduces its evaluation time from square of the number of species to a linear dependence.

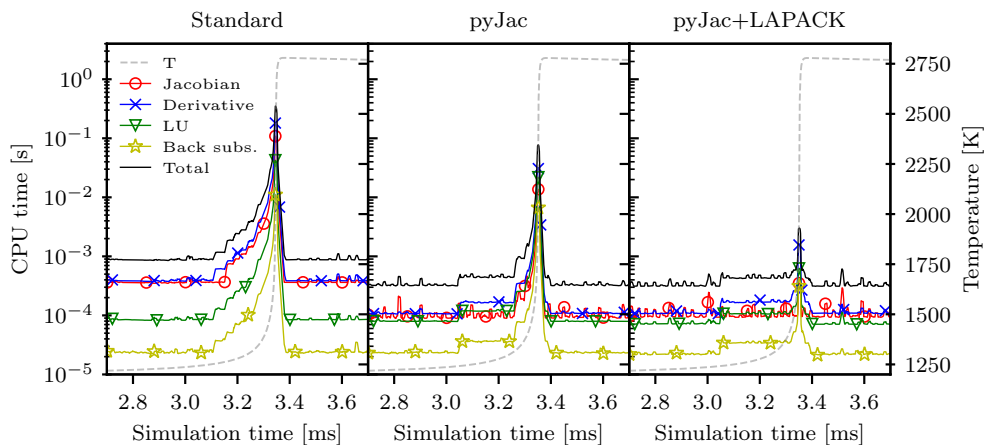


Figure 2: CPU time spent on different operations of ODE solution algorithm for a single cell 0D problem involving CH_4 chemistry using **Standard**, **pyJac** and **pyJac+LAPACK** models. Selected timeframe represents the most computationally demanding part of the problem. The GRI-3.0 mechanism (53 species and 325 reactions) is used in the benchmark.

OpenFOAM features a fully algebraic Jacobian implementation to speed up the solution of chemical kinetics in its recent releases [36]. However, we have found that the implemented algebraic Jacobian fails to deliver a fast solution to chemistry ODE integration when high ODE convergence tolerances are utilized. Instead, we utilize the python-based open-source software **pyJac**, introduced by Niemeyer et al. [26]. The **pyJac** package generates C subroutines for evaluation of an analytical Jacobian for a chemical mechanism. They reported that **pyJac** performs 3 to 7.5 times faster than the first-order finite differencing approach. In our proposed model, OpenFOAM’s Jacobian calculation subroutines are replaced with the subroutines generated by **pyJac**.

The fully algebraic Jacobian utilization via **pyJac** speeds up the Jaco-

bian evaluation time and improves the solution convergence rate. However, the ODE solution method itself is also particularly important for obtaining faster chemistry solution. We observed that the OpenFOAM’s native functions used for LU decomposition and back substitution matrix operations of the chemistry ODE system are not suitable for solving dense and small matrices ($<500 \times 500$). Therefore the LU decomposition and back substitution linear algebraic operations of OpenFOAM are replaced by the more robust implementations existing in the open-source library LAPACK [32]. The LAPACK routines utilized in our model are very efficient for dense and small matrices, such as the fully dense Jacobian matrix created by the `pyJac`.

In this study, LAPACK functions were linked to a semi-implicit extrapolation-based Euler method, denoted as Seulex [21, 35]. Seulex requires the specification of relative and absolute tolerances of the solution along with an initial estimate of Δt_{ODE} . As the solution progresses, the solver improves the estimate for Δt_{ODE} at the current thermochemical state using theoretical relations and heuristics. The previous available value is then used as an initial value for the following integration interval. Furthermore, a Δt_{ODE} is recursively split into a number of partitions and each partition is then solved using a low-order method. Finally, the high-order solution over the whole interval Δt_{ODE} is recursively gathered from solutions of the smaller partitions. If the solution does not satisfy the tolerance criteria, partitioning continues until it is satisfied. A more detailed explanation of the Seulex algorithm can be found in the work by Imren and Haworth [35].

As noted earlier, each computational cell has its own independent ODE problem with a thermochemical state vector comprising only intensive mix-

ture properties. Furthermore, the ODE solver guarantees that if the solution has converged, the error will lie within user-specified tolerance regardless of the width of the integration interval Δt_{CFD} . However, the error related to the operator splitting technique needs to be taken care of. The assumption behind the operator splitting is that the chemistry timescales are orders of magnitude smaller than the flow timescales or the CFD solver time step Δt_{CFD} . Nevertheless, the time step Δt_{CFD} is to be chosen so that the species and temperature transport effects over a time step are accounted for and the thermochemical state vector is updated correspondingly. We note that in this study we do not consider any chemical source term closures for the filtered or averaged equations. Such turbulence-chemistry interaction (TCI) models could significantly depend on the mesh parameters and the CFD time step size and might require a separate treatment.

The effect of the optimized Jacobian evaluation is demonstrated in Figure 2 on a 0-dimensional (0D) homogeneous reactor simulation with stoichiometric methane-air mixture at $T = 1200$ K and $p = 13.5$ atm. The GRI-3.0 [37] chemical kinetic mechanism was used and the absolute and relative ODE solver tolerances were set to 10^{-10} and 10^{-6} , respectively. The integration interval (Δt_{CFD}) was fixed to 10^{-6} s which corresponds to timescales relevant to reactive CFD applications under engine-relevant conditions. From the figure, it is observed that the time spent on Jacobian and derivative evaluations is reduced by roughly one order of magnitude between `Standard` and `pyJac` along the entire simulation time. Furthermore, the exact Jacobian formulation increases the solution accuracy for every Newton iteration, which reduces the amount of iterations required for convergence. Next, with `LAPACK`

we notice a further reduction in the analytical Jacobian retrieval and also less time for all operations only within the sharp gradient zone. The reason is that with LAPACK the ODE solver uses wider sub-interval in the stiff zone, hence, fewer function calls for the Jacobian retrieval and consequently, fewer linear algebraic operations.

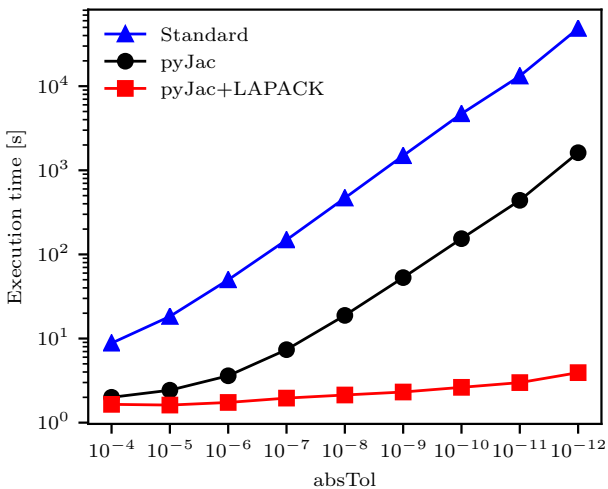


Figure 3: Dependency of the execution time on the absolute tolerance ($N_{sample} = 10$) for a single cell 0D problem involving CH_4 chemistry with different ODE convergence tolerances. The GRI-3.0 mechanism (53 species and 325 reactions) is used in the benchmark.

Figure 3 depicts the total execution times for the aforementioned problem with varied absolute tolerances. It can be seen that while the Jacobian retrieval using pyJac reduces the execution time by about one order of magnitude, using LAPACK routines provides another order of magnitude speed-up. Utilization of pyJac together with LAPACK allows using much tighter ODE tolerances.

3. Results

3.1. An overview of the test cases

After the introduction of the new features of our model in the previous section, here the combined effect of the DLBFoam library with pyJac and LAPACK is investigated. Three different models are employed here for performance benchmarking: 1) the standard OpenFOAM chemistry model (referred to as **Standard**), 2) our original model with dynamic load balancing and zonal reference mapping [4] (referred to as DLBFoam), and 3) our original model combined with the ODE related improvements utilizing pyJac and LAPACK routines (referred to as DLBFoam+pyJac). We first demonstrate the computational performance of DLBFoam+pyJac in two academic test cases (2D reacting shear layer and 3D stratified combustion). After that, we demonstrate its performance in two experimental flame configurations (ECN Spray A and Sandia flame D). Schematic diagrams presenting the four test cases are provided in Figure 4.

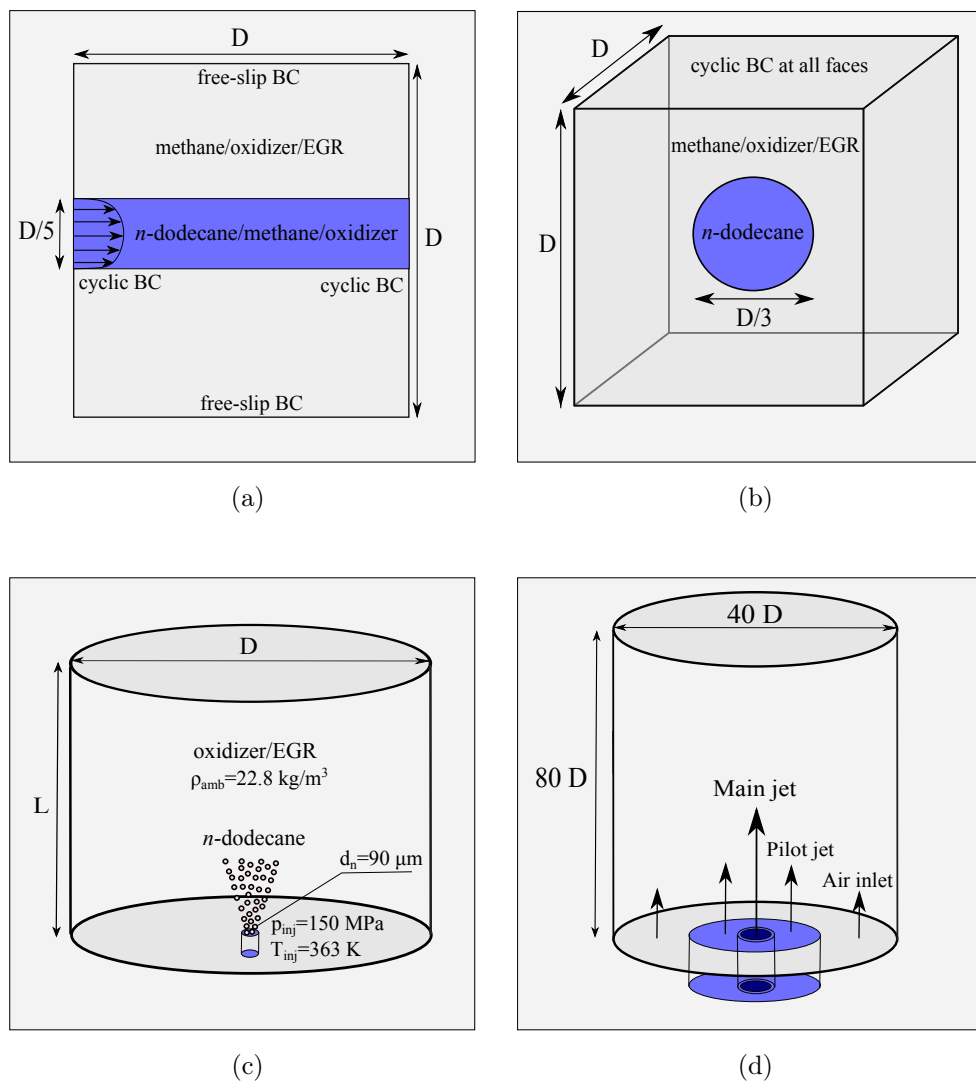


Figure 4: Schematic diagrams of the demonstrated test cases. (a) 2D reacting shear layer, (b) 3D stratified combustion, (c) ECN Spray A, (d) Sandia flame D.

For each case, we first use DLBFoam+pyJac to solve a full-scale combustion problem. Then, for each problem we choose a time interval which is considered computationally challenging, e.g., chemistry ODE problem is stiff

in parts of the domain due to ignition, and compare the performance of DLBFoam+pyJac against DLBFoam and Standard for a specific number of iterations. A summary of various case-specific benchmark parameters along with computational speed-up are presented in Table 1. Here, we have to limit the number of iterations for benchmarking because of the poor performance of the Standard model we highlighted in the previous section. In fact, with the chosen strict tolerance values, it is infeasible to carry out a full simulation with Standard or even benchmark with a larger number of iterations than those stated in the table for all of the studied test cases.

Table 1: List of parameters used in performance benchmarks. Computational time refers to the full-scale simulation using DLBFoam+pyJac. Computational speed-up is reported for DLBFoam+pyJac against Standard. Computational time for ECN Spray A reports the case with $T_{amb} = 900$ K and simulation time of 1.5 ms.

	2D shear layer	3D stratified combustion	ECN Spray A	Sandia flame D
Chemical mechanism	Yao [38]	Yao	Yao	DRM19 [39]
Number of cells	90 000	16.78M	39M	1.99M
Number of processors	8–32	1152	1920	768
Benchmarking samples (CFD iterations)	100	7	65	100
Computational speed-up	24–38	≈ 400	256	13.5
Computational time [CPU-hr]	65	15 000	128 500	24 500

Regarding numerical schemes, a second-order spatial and temporal discretization is utilized for all test cases presented herein. The reacting PISO (Pressure-Implicit with Splitting of Operators) algorithm with two outer-loop correctors is utilized for pressure-velocity coupling [40], i.e., chemistry is solved twice within a single CFD time step. The absolute and relative tolerances of the chemistry ODE solver are set to 10^{-10} and 10^{-6} , respectively.

More details about the case setups can be found in test case files which are openly shared [41].

All simulations and benchmarks were performed on the Mahti supercomputer at CSC - Finnish IT Center for Science. Mahti has 1404 nodes each with two 64-core 2.6 GHz (boost up to 3.3 GHz) AMD Rome 7H12 CPUs. All nodes are connected to the inter-node communication network with 200 GB/s links [42].

3.2. 2D reacting shear layer

The first test case presents a simple, temporally evolving 2D reacting shear layer which is computationally affordable even on a personal computer. The presented test case is fundamentally related to the ignition and flame initiation of DF combustion in compression-ignition engines such as the reactivity controlled compression ignition (RCCI) engine [33, 43]. We demonstrate the computational speed-up and scaling effects of DLBFoam+pyJac with respect to the number of cores.

The schematic of the present numerical setup is illustrated in Figure 4a. The setup contains a high reactivity *n*-dodecane jet stream that mixes with the surrounding oxidizer consisting of premixed methane, oxidizer and exhaust gas recirculation (EGR). The simulation domain is a square box with a side length $D = 1.5$ mm. The number of grid points in both directions is 300 which is based on the pre-estimated laminar flame thickness for *n*-dodecane-methane premixed flame at the corresponding most reactive mixture fraction, $p = 60$ bar, and $T_{\text{reactants}} = 800$ K ($\delta_f \approx 50$ μm) to resolve the flame by 10 grid points. A hyperbolic tangent function is used to generate the shear layer between the *n*-dodecane and oxidizer streams. The *n*-dodecane jet is initially

set to 700 K whereas the methane/air mixture is set to 900 K at a constant pressure of 60 bar. The initial conditions corresponding to the ambient premixed mixture are similar to our previous DF spray studies [33, 43–47] as reported in Table 2. The *n*-dodecane jet moves initially with a relative velocity of 10 m/s to the methane/air stream and develops a Kelvin-Helmholtz instability. A skeletal chemical mechanism (54 species and 269 reactions) developed by Yao et al. [38] for *n*-dodecane combustion is used. The performance of this mechanism in DF context has been already demonstrated in our earlier studies [33, 44, 46].

Table 2: Initial conditions in molar fractions and corresponding equivalence ratio for premixed ambient mixture in 2D shear layer and 3D stratified combustion cases.

CH ₄ %	O ₂ %	CO ₂ %	H ₂ O %	N ₂ %	ϕ_{CH_4}
3.750	15	5.955	3.460	71.835	0.5

Figure 5 highlights the DF ignition process in the shear layer, where *n*-dodecane jet ignites the surrounding mixture. It is observed that the first-stage ignition from low-temperature chemistry develops primarily within the *n*-dodecane jet near the mixing layer. Next, the ignition front initiates in the *n*-dodecane region at the most reactive mixture fraction and propagates towards the ambient mixture. Here, the mixture fraction describes the mixing extent of *n*-dodecane fuel stream and the premixed methane, oxidizer and EGR. Finally, a premixed flame front is established which completes the combustion of the ambient methane.

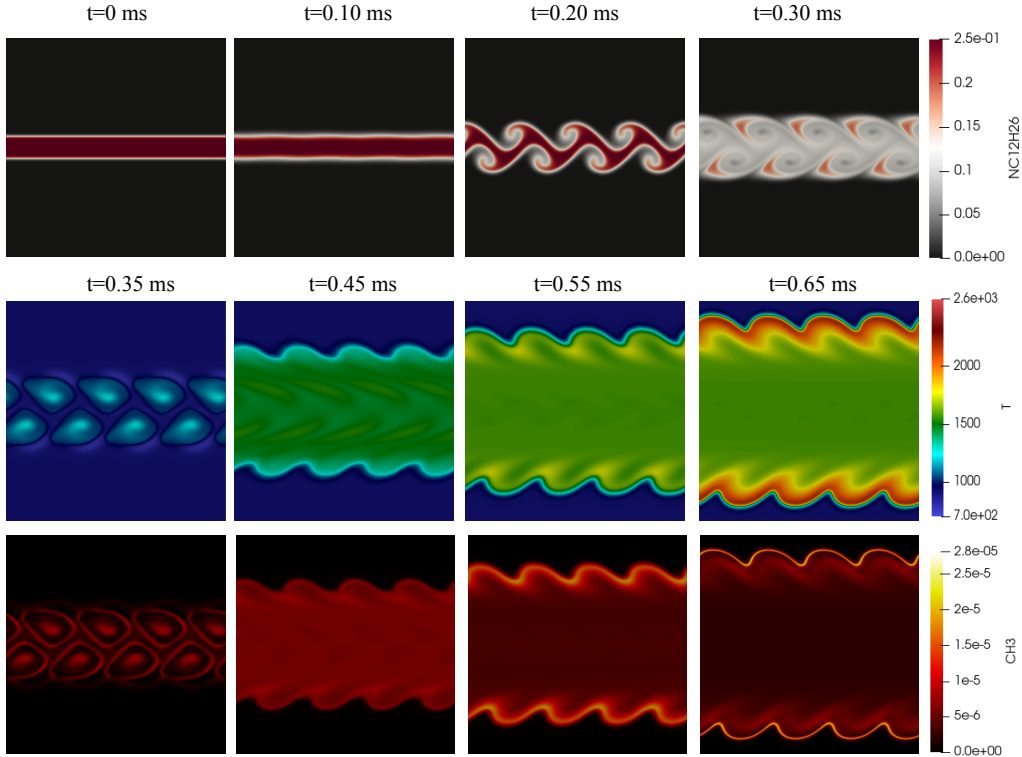


Figure 5: Temporal evolution of *n*-dodecane (top row), temperature (middle row), and CH_3 (bottom row) fields of the 2D reacting shear layer simulation, where the *n*-dodecane jet initiates the flame and then burns the premixed ambient.

Next, we report the computational speed-up and the parallel efficiency provided by our model for different processor counts, as depicted in Figure 6. The domain is decomposed into 8, 16, and 32 processors to demonstrate the scaling capabilities of the model. All speed-up tests are carried for 100 constant CFD time steps of 2×10^{-7} s after the DF ignition. The following observations are made from the analysis: 1) the **Standard** model demonstrates a poor parallel scaling efficiency due to the load imbalance. While the strong scaling efficiency of **DLBFoam** and **DLBFoam+pyJac** are almost linear ($> 95\%$),

the **Standard** shows a scaling efficiency around 75% for the investigated processor counts. This explains the increased speed-up value for DLBFoam and DLBFoam+pyJac for higher processor counts. 2) The DLBFoam model provides speed-up by a factor of 1.71 to 2.89 for different processor counts, compared to **Standard**. 3) The DLBFoam+pyJac model provides speed-up by a factor of 23.98 to 38.07 compared to **Standard**.

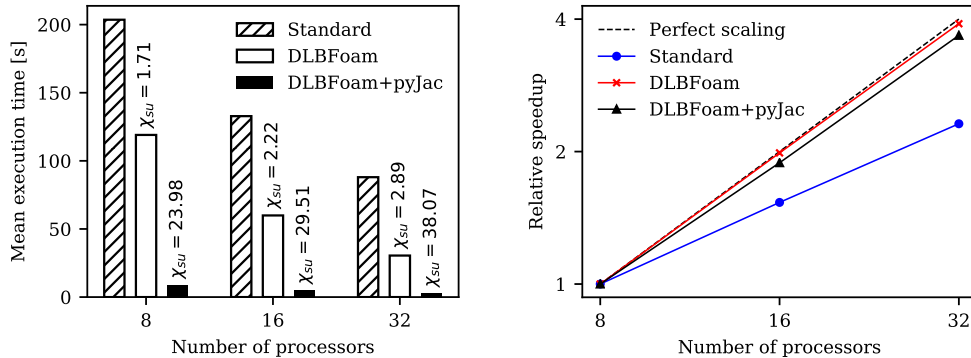


Figure 6: Left: Mean execution times over 100 iterations for the 2D reacting shear layer for different number of processors. Here, χ_{su} is the speed-up factor of DLBFoam or DLBFoam+pyJac compared to **Standard**. Right: Speed-up values for different number of processors relative to 8 processors case.

3.3. 3D stratified combustion

After providing speed-up benchmarks along with scaling tests in the previous section, we next present another academic test case in this section, i.e. 3D stratified combustion (Figure 7). This case can not be even tested for 10 iterations using **Standard** within a reasonable computational time. Hence, the purpose here is mainly to show that it is possible to investigate 3D ignition/combustion problems using DLBFoam+pyJac. This DF test case has close relevance to combustion mode design in modern engines such as RCCI.

This test case is conceptually similar to the previous 2D setup by Karimkashi et al. [48]. As shown in the schematic Figure 4b, the computational domain is a 3D cube with periodic boundary conditions and a side length $D = 1$ mm. The grid size is $4\ \mu\text{m}$ with 256 grid points along each direction, to capture the flame with at least 10 grid points within the laminar flame thickness ($\delta_f \approx 40\ \mu\text{m}$). The initial pressure is set at 60 bar and the initial temperature is homogeneous within the entire computational domain at 800 K, which is relevant to the estimated temperature at the most reactive mixture fraction for DF methane/*n*-dodecane based on 0D simulations [44, 46, 47, 49]. Here, pure *n*-dodecane is initially constrained in a blob in the middle of the domain with a diameter $d = D/3$. The ambient gas consists of premixed methane, oxidizer and EGR at $\phi_{\text{CH}_4} = 0.5$, similar to the previous test case, with the composition reported in Table 2. As in the previous test case, Yao mechanism is used.

Turbulence is initialized using Taylor-Green-Vortex (TGV) structure, which is generated in a separate non-reactive 3D simulation with an initial velocity $U = 50$ m/s and reference length $L_{\text{ref}} = D/2\pi$. We let the initialized TGV to evolve in time until the gradient of total kinetic energy reaches its peak and then, velocity and pressure fields are mapped to the reactive case as initial fields. The estimated Reynolds number at the start of reacting simulation is $Re \approx 1000$. In this case study, the interactive roles of convection, diffusion and reaction are investigated. First, the initial *n*-dodecane is mixed with the ambient gas at early simulation time instances, long before the second-stage ignition (τ_2). Here, $\tau_2 \approx 0.28$ ms is defined as the first time instance when $T > 1500$ K. At τ_2 , the stratified mixture ignites at the most reactive

mixture fractions. The ignition front propagates and finally forms laminar premixed flame fronts, which complete the combustion in the standard deflagration mode. The present observations in 3D are in close agreement with the observations made in our previous study in 2D [48].

Figure 7 depicts 2D cut-planes for temporal evolution of temperature (top row), *n*-dodecane (second row), methane (third row), and hydroxyl radical OH (bottom row) wherein time is normalized by τ_2 . It is observed that a stratified mixture of *n*-dodecane and methane/oxidizer is formed before any significant temperature rise in the system ($t = 0.7\tau_2$). Closer to the ignition time, hot spots emerge ($t = 0.9\tau_2$) and deflagrative-like fronts develop at a moderate rate with various wrinkled surfaces ($t = 1.1\tau_2$). Slightly after the ignition time, the fronts evolve ($t = 1.3\tau_2$) as clearly observed from the OH cutplane. Finally, the fronts merge ($t = 1.8\tau_2$) and combustion is almost complete. We note that at $t = 1.8\tau_2$, only small fractions of *n*-dodecane and methane are left in the system, which are convected from other iso-surfaces to the displayed cutplane in Figure 7.

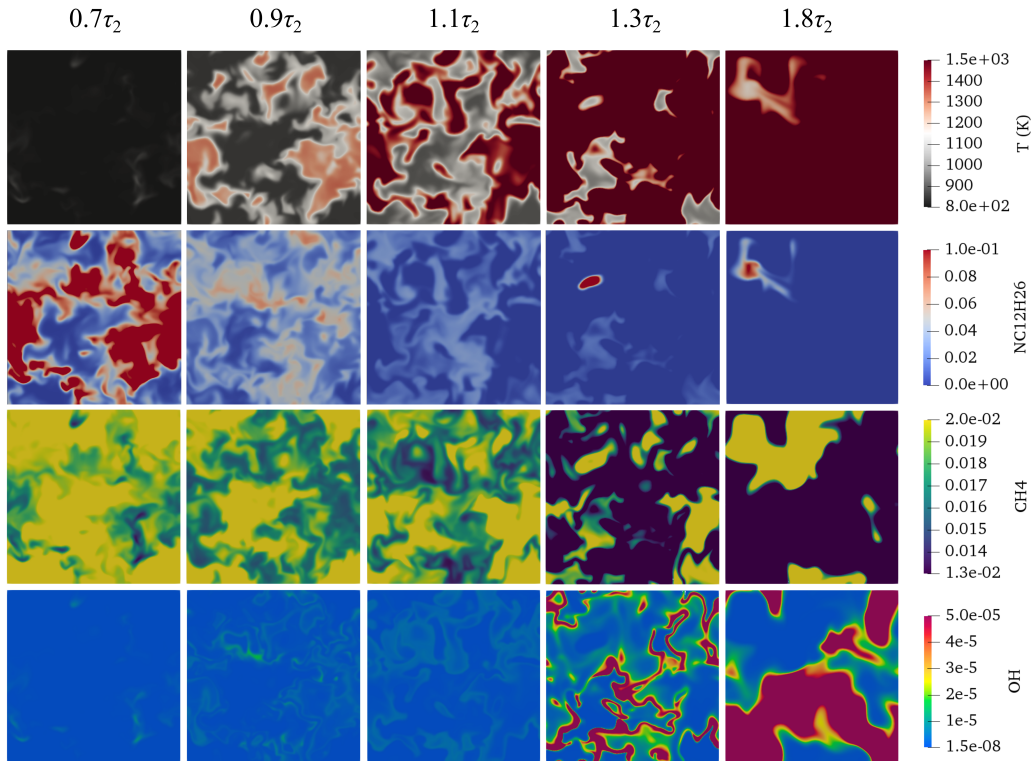


Figure 7: Temporal evolution of temperature (top row), *n*-dodecane (second row), methane (third row), and OH (bottom row) are shown in cutplanes taken from the 3D stratified combustion simulation around the second-stage ignition time. With gradual temperature rise, ignition kernels are formed at different locations. Consistently, the fuels (*n*-dodecane and methane) are consumed and deflagrative-like fronts are formed and finally merged.

In this case study, a speed-up gain by a factor of 2 to 3 orders of magnitude is observed with DLBFoam+pyJac compared to `Standard`. Therefore, it would not be possible to benchmark this problem using `Standard` for 100 iterations. In particular, we evaluate the speed-up of our model against `Standard` by restarting the simulation from the first-stage ignition time (0.2 ms) and using the same number of processors (1152 processors) and identical toler-

ances. While `Standard` simulation proceeds only 7 iterations in ~ 76000 seconds of clock time, the respective time is only about 200 seconds with `DLBFoam+pyJac`; i.e. speed-up by a factor of ≈ 400 with `DLBFoam+pyJac` compared to `Standard` is achieved. As a final note, the total clock time for simulating this case using `DLBFoam+pyJac` with 1152 processors for 0.5 ms simulation time is ≈ 13 hours. Hence, `DLBFoam+pyJac` is a key enabler to study such 3D reactive flow configurations with OpenFOAM.

3.4. ECN Spray A

At this point, it is clear that `DLBFoam+pyJac` offers great advantages over `Standard`. In particular, `DLBFoam+pyJac` was shown to scale almost linearly with the number of processors in an academic case and enable 3D reactive simulations with a relatively large chemical kinetic mechanism and tight solver tolerances. Next, we move on to a more realistic 3D configuration i.e. the Engine Combustion Network Spray A test case with experimental validation data. Spray A represents an igniting non-premixed diffusion flame under engine-relevant conditions. Hence, it is an optimal test case for reactive CFD large-eddy simulation (LES) code validation.

A schematic of the computational setup is demonstrated in Figure 4c, where the domain volume corresponds to that of ECN combustion vessel by Sandia. Liquid *n*-dodecane at temperature of 363 K and pressure of 150 MPa is injected from a 90 μm nozzle (i.e. Spray A) into a hot quiescent ambient gas of density 22.8 kg/m³ and mixture composition (15% O₂, 75.15% N₂, 6.23% CO₂ and 3.62% H₂O) based on the molar fractions. The simulations are performed for 4 reacting cases with varied ambient temperature (900, 1000, 1100, and 1200 K), and a single non-reacting case at 900 K. The

domain is discretized with static mesh of $62\ \mu\text{m}$ cell size in the inner most refinement layer to resolve the turbulent mixing and the quasi-steady lifted flame, as shown in Figure 8, resulting in total amount of 25–39 million cells depending on the particular case. Moreover, the implicit LES (ILES) approach is employed for turbulent subgrid-scale (SGS) modeling, consistent with our previous spray combustion works [27, 44–47, 50, 51], while the no-breakup model approach is used for droplet atomization which is further discussed by Gadalla et al. [51]. The volume-rendered spray flame shown in Figure 8 for ambient $T = 900\ \text{K}$ indicates the mixing and evaporation zone, the low-temperature combustion zone, and the ignition and high temperature combustion region wherein fully developed diffusion flame is observed.

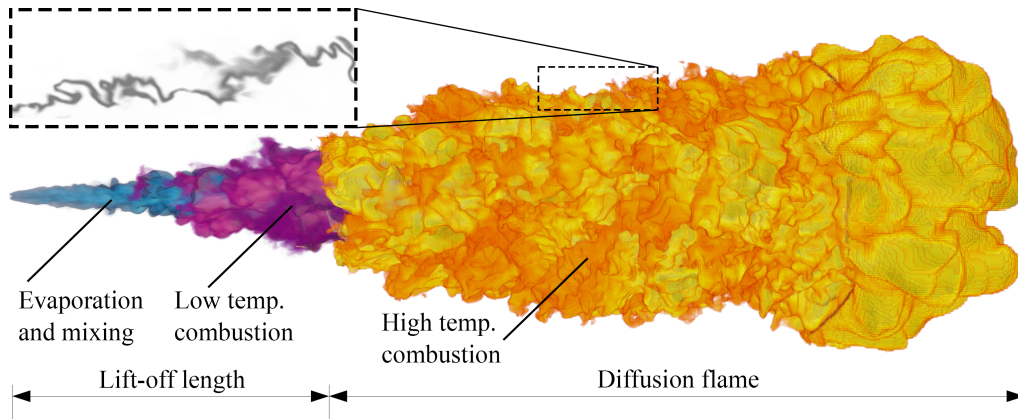


Figure 8: Volume rendering of the ECN Spray A diffusion flame of ambient $T = 900\ \text{K}$ after 1.5 ms. The inset in the top left corner presents a 2D projected cut-plane of the OH radical mass fraction.

The present show case demonstrates the capability of our new model to match the well-known ECN Spray A benchmark. First, in Figure 9a liquid and vapor penetrations are validated against experimental data up

until 1.5 ms under non-reacting conditions at 900 K. Then, the simulation is repeated in reacting mode and the pressure rise is monitored in Figure 9b against experiments for the same temporal interval. In Figure 9c the formaldehyde (CH_2O) planar laser-induced fluorescence (PLIF) false color images obtained by Skeen et al. [52] at various snapshots are compared against the corresponding LES data using the new solver. Here, the LES data are circumstantially averaged for each sampling point in the axial-radial plane, which are then compared with the experimental data set. This comparison verifies the global trends for Spray A baseline including ignition onset, cool flame, and quasi-steady flame lift-off. Finally, validations of ignition delay times (IDTs) and flame lift-off lengths against experimental data at various temperature levels are presented in Figure 9d.

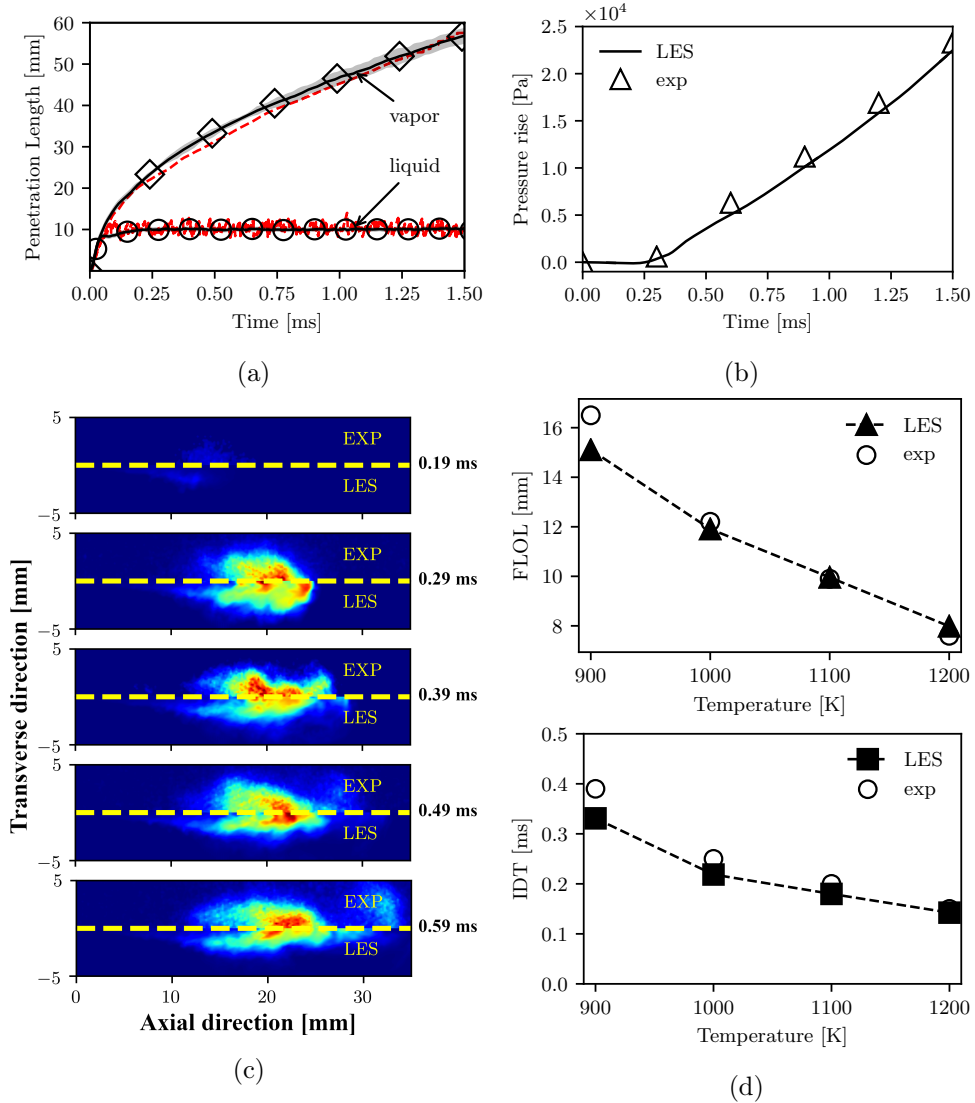


Figure 9: Validations of the ECN Spray A at ambient $T = 900$ K for (a) liquid and vapor penetrations under non-reactive conditions, (b) pressure rise in the combustion vessel after ignition, (c) formaldehyde fields at various snapshots, and (d) ignition delay time and flame lift-off length (FLOL) at varied ambient temperature levels of the mixture.

After that, we demonstrate in Figure 10 the gained speed-up using DLBFoam+pyJac

within 100 time steps after 0.3 ms of the simulation and using a constant step size of 2×10^{-7} s. The load imbalance in this test case is rather high. It originates from the large number of ambient cells which are computationally less stiff than those in the ignition region. This imbalance is further increased with reference mapping so that ambient cells become mostly idle, hence improving the performance gain of dynamic load balancing, which results in a factor of 38 speed-up, compared with **Standard**. After that, a further speed-up by a factor of 6.7 is attributed to the analytical Jacobian retrieval and the robust linear algebra, i.e. **DLBFoam+pyJac**, hence a total speed-up by a factor of 256 as compared to **Standard**.

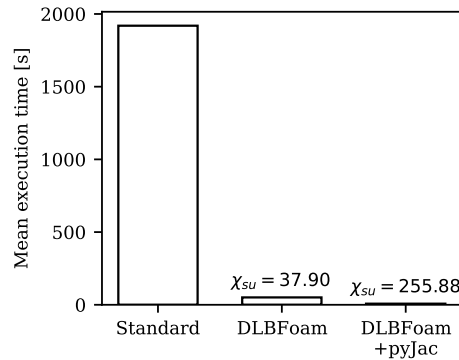


Figure 10: Mean execution times over 65 iterations for the ECN Spray A after 0.3 ms of the simulation. χ_{su} is the speed-up factor of **DLBFoam** or **DLBFoam+pyJac** compared to **Standard**.

3.5. Sandia flame D

The ECN Spray A case demonstrated excellent performance for LES of non-premixed spray flame using **DLBFoam+pyJac**. The last test case is the Sandia flame D [53] representing a piloted partially premixed methane-air

flame. Sandia flame D is a well-known configuration from the TNF workshop flame series, which is often studied in the literature, e.g. [54–57]. Therefore, it is considered as a useful benchmark for reactive CFD LES code validation for gas burner flame investigations.

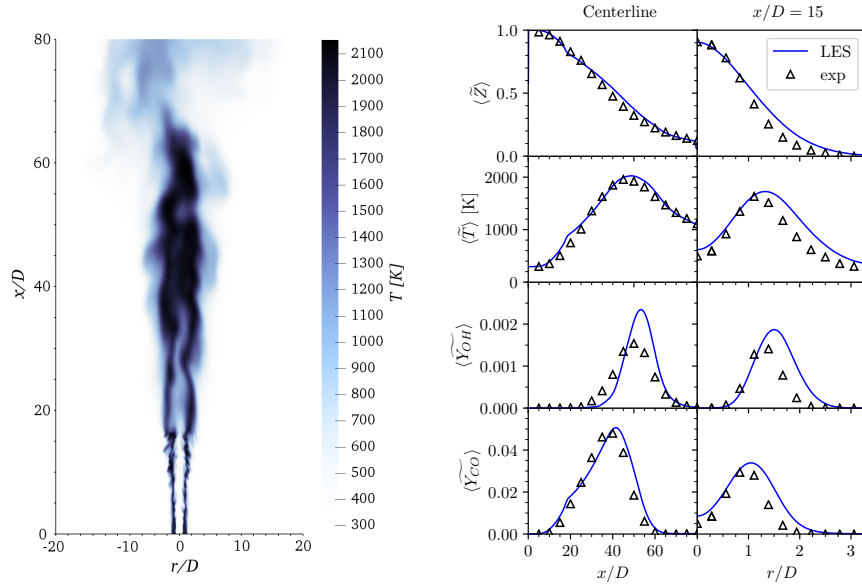


Figure 11: Top: Instantaneous temperature field of Sandia flame D at $t = 0.1$ s. Note that the data attributed to the refined grid is only available to $x/D = 15$ in order to limit the computational cost. Bottom: Validations of the Sandia flame D for mean mixture fraction, temperature and species mass fraction at centerline and $x/D = 15$.

A schematic of the Sandia flame D setup is provided in Figure 4d. The main jet is a mixture of CH_4 and air at equivalence ratio $\phi_{\text{CH}_4} = 3.17$. It is injected with a bulk velocity of 49.6 m/s and temperature of 294 K to the domain from a nozzle of diameter $D = 7.2$ mm. The flame is stabilized with a pilot jet which is a hot (1880 K) lean mixture of C_2H_2 , H_2 , air, CO_2 and N_2 . The inner and outer diameters of the pilot nozzle are 7.7 mm and 18.2 mm,

respectively, and the flow velocity is 11.4 m/s. Jet inlets are surrounded by air co-flow with an inner diameter of 18.9 mm. A Cartesian mesh is used, and a refinement zone with cell size of $0.75 \text{ mm} \times 0.368 \text{ mm} \times 0.368 \text{ mm}$ defined from the nozzle exit until $15D$ is realized, resulting in a total of $2M$ cell count. Velocity fluctuations in the form proposed by Pitsch and Steiner [54] are superimposed on the main jet inlet velocity profile to induce turbulent jet behaviour. Here, the purpose is to demonstrate that the code produces first order statistics for this flame configuration. Hence, we do not focus on the turbulence-chemistry interaction modeling but use the ILES approach as a SGS scale model, consistent to the previous test cases. A reduced chemical kinetic mechanism DRM19 [39] with 21 species and 83 reactions is used. The simulation is performed for 100 ms after which the fields are averaged for another 150 ms, where the flame becomes statistically stable.

Figure 11 depicts time-averaged mixture fraction, temperature and specie mass fractions profiles compared to the experimental data [53] and an instantaneous snapshot of the temperature field. The close agreement between experiments and predicted mixture fraction and temperature profiles along the center axis indicates that the coupled influence of turbulent mixing and flame heat release is resolved adequately in the core of the jet flame. Minor species profiles, CO and OH, also correspond well with the experiments. Predicted OH mass fractions show correct trends, however the maximum value is overpredicted compared with the measured data. Overall, mass fraction prediction of short lived species like OH is a challenging task due to the nonlinear evolution of the species [55–58] and it is out of the scope of the present study. In the radial direction, the reactions are mostly occurring in

the shear layer between the main jet and co-flow ($r/D = 1$), which is evident in the peaks of the mass fraction profiles. The radial profiles agree well with the experimental data on the rich side. However, mixing is overpredicted in the lean region ($r/D > 1$). Close to the nozzle and away from the central axis, the reaction zone may still be considered relatively laminar [54]. Therefore, the overpredicted profiles in the lean region could be explained by the utilized unity Lewis number assumption. Moreover, the temperature and species profiles also follow the same trend as the mixture fraction in the flame on the rich and lean sides.

Next, a speed-up test is carried out for a stabilized flame for 100 iterations with a constant time step of 1×10^{-6} s. The results are presented in Figure 12. The `DLBFoam` provides speed-up by a factor of 4.52, which is significantly lower than with ECN Spray A. This can be explained by a relatively low number of mapped cells due to the location of the refinement zone in the core of the jet. Optimized ODE solver routines `pyJac` and `LAPACK` bring additional speed-up by a factor of 2.99. Here, the lower speed-up is a consequence of the use of the reduced mechanism, which as discussed earlier significantly reduces computational cost of the chemistry problem. However, the combined effect of the `DLBFoam+pyJac` is significant and brings about 1 order of magnitude speed-up to this case.

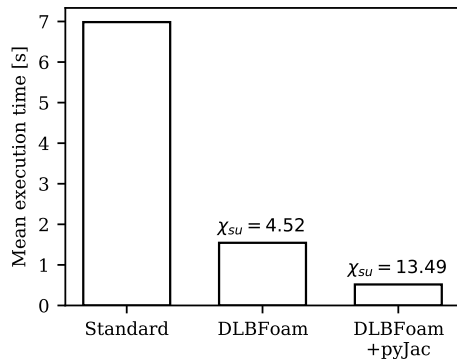


Figure 12: Mean execution times over 100 iterations for the Sandia flame D after 0.1 s of the simulation. χ_{su} is the speed-up factor of DLBFoam or DLBFoam+pyJac compared to Standard.

4. Conclusions

In this work, an open-source dynamic load balancing library for OpenFOAM, namely DLBFoam, with reference mapping feature was re-introduced and improved. In particular, the feature was extended with optimized chemistry ODE solution routines. First, the Jacobian evaluation procedures in OpenFOAM were replaced with an analytical implementation provided by the open-source package pyJac. This step resulted in one order of magnitude speed-up in a 0D homogeneous reactor test case. Then in order to fully utilize the benefits of the new fully dense Jacobian, LU decomposition and back substitution routines were replaced with more robust ones from the open-source library LAPACK, resulting in even higher speed-up especially for tighter ODE tolerances.

The improvements were tested in two academic cases and then applied to two experimental flame cases. First, the model was tested in a 2D reacting

shear layer problem, demonstrating almost perfectly linear scaling. Speed-up by a factor of ≈ 30 was demonstrated in the 2D case for DLBFoam with pyJac and LAPACK. Second, 3D stratified combustion was studied, which was not even computationally feasible to benchmark with the Standard model due to 2–3 orders of magnitude performance difference. Last, two 3D flames were investigated: ECN Spray A and Sandia Flame D showing speedup factors of ≈ 256 and ≈ 13.5 respectively for DLBFoam with pyJac and LAPACK. We also note that the reported speed-up numbers in comparison to Standard were achieved with fixed ODE tolerances, specific time step sizes, and chemical kinetic mechanisms. It is worth acknowledging that changing those parameters may affect the speed-up estimates. However, the promising results herein indicate that the improvements to DLBFoam offer an avenue to model complex combustion phenomena in OpenFOAM with increased accuracy and computational efficiency. Further investigations in a broader user community could result in more in-depth analysis and development of the present test cases for different combustion models and chemical mechanisms. As future work, more test cases could be established around the proposed reactive CFD approach to account for a broader variety of turbulent combustion conditions. Finally, the source code and the case setup files used in this work are openly available [41, 59]

Acknowledgements

This study is financially supported by the Academy of Finland (grant numbers 318024, 332784, and 332835). Computational resources have been provided by CSC – Finnish IT Center for science and Aalto Science-IT

project. We gratefully thank Dr. Heikki Kahila (Wärtsilä Finland Oy) and Dr. Petteri Peltonen (VTT Oy) for their precious comments and technical advice throughout the implementation process.

Appendix A. Supplementary material

Library source code is openly available in a public GitHub repository [59]. Test case setups are openly available in a separate public GitHub repository [41].

References

- [1] exaFoam project overview, <https://exafoam.eu/overview/>, accessed: 2021-10-21.
- [2] T. Poinsot, D. Veynante, Theoretical and Numerical Combustion, 3rd Edition, Authors, 2011.
- [3] N. Peters, Turbulent Combustion, Cambridge Monographs on Mechanics, Cambridge University Press, 2000. doi:10.1017/cbo9780511612701.
- [4] B. Tekgül, P. Peltonen, H. Kahila, O. Kaario, V. Vuorinen, DLBFoam: An open-source dynamic load balancing model for fast reacting flow simulations in OpenFOAM, Computer Physics Communications 267 (2021) 108073. doi:10.1016/j.cpc.2021.108073.
- [5] D. Kochkov, J. A. Smith, A. Alieva, Q. Wang, M. P. Brenner, S. Hoyer, Machine learning–accelerated computational fluid dynamics, Proceed-

- ings of the National Academy of Sciences 118 (21) (2021) e2101784118. doi:10.1073/pnas.2101784118.
- [6] M. Gadalla, M. Cianferra, M. Tezzele, G. Stabile, A. Mola, G. Rozza, On the comparison of LES data-driven reduced order approaches for hydroacoustic analysis, *Computers & Fluids* 216 (2021) 104819. doi:10.1016/j.compfluid.2020.104819.
- [7] S. Hijazi, G. Stabile, A. Mola, G. Rozza, Data-driven POD-Galerkin reduced order model for turbulent flows, *Journal of Computational Physics* 416 (2020) 109513. doi:10.1016/j.jcp.2020.109513.
- [8] N. Wandel, M. Weinmann, R. Klein, Teaching the incompressible Navier–Stokes equations to fast neural surrogate models in three dimensions, *Physics of Fluids* 33 (4) (2021) 047117. doi:10.1063/5.0047428.
- [9] Z. Li, Y. Ju, C. Zhang, Parallel large eddy simulations of transitional flow in a compressor cascade with endwalls, *Physics of Fluids* 31 (11) (2019) 115104. doi:10.1063/1.5123034.
- [10] S. Brahmachary, A. Bhagyarajan, H. Ogawa, Fast estimation of internal flowfields in scramjet intakes via reduced-order modeling and machine learning, *Physics of Fluids* 33 (10) (2021) 106110. doi:10.1063/5.0064724.
- [11] S. J. Plimpton, S. G. Moore, A. Borner, A. K. Stagg, T. P. Koehler, J. R. Torczynski, M. A. Gallis, Direct simulation Monte Carlo on petaflop

- supercomputers and beyond, *Physics of Fluids* 31 (8) (2019) 086101. doi:10.1063/1.5108534.
- [12] V. Sekar, Q. Jiang, C. Shu, B. C. Khoo, Fast flow field prediction over airfoils using deep learning approach, *Physics of Fluids* 31 (5) (2019) 057103. doi:10.1063/1.5094943.
- [13] G. Aversano, G. D'Alessio, A. Coussement, F. Contino, A. Parente, Combination of polynomial chaos and Kriging for reduced-order model of reacting flow applications, *Results in Engineering* 10 (2021) 100223. doi:10.1016/j.rineng.2021.100223.
- [14] A. Wehrfritz, O. Kaario, V. Vuorinen, B. Somers, Large Eddy Simulation of n-dodecane spray flames using Flamelet Generated Manifolds, *Combustion and Flame* 167 (2016) 113–131. doi:10.1016/j.combustflame.2016.02.019.
- [15] V. Jaganath, M. Stoellinger, Transported and presumed probability density function modeling of the Sandia flames with flamelet generated manifold chemistry, *Physics of Fluids* 33 (4) (2021) 045123. doi:10.1063/5.0045726.
- [16] F. Contino, H. Jeanmart, T. Lucchini, G. D'Errico, Coupling of in situ adaptive tabulation and dynamic adaptive chemistry: An effective method for solving combustion in engine simulations, *Proceedings of the Combustion Institute* 33 (2) (2011) 3057–3064. doi:10.1016/j.proci.2010.08.002.

- [17] T. Lu, C. K. Law, Toward accommodating realistic fuel chemistry in large-scale computations, *Progress in Energy and Combustion Science* 35 (2) (2009) 192–215. doi:10.1016/j.pecs.2008.10.002.
- [18] C. K. Law, Combustion at a crossroads: Status and prospects, *Proceedings of the Combustion Institute* 31 I (1) (2007) 1–29. doi:10.1016/j.proci.2006.08.124.
- [19] Y. Pei, M. Mehl, W. Liu, T. Lu, W. J. Pitz, S. Som, A multicomponent blend as a diesel fuel surrogate for compression ignition engine applications, *Journal of Engineering for Gas Turbines and Power* 137 (11) (nov 2015). doi:10.1115/1.4030416.
- [20] S. M. Sarathy, G. Kukkadapu, M. Mehl, T. Javed, A. Ahmed, N. Naser, A. Tekawade, G. Kosiba, M. AlAbbad, E. Singh, S. Park, M. A. Rashidi, S. H. Chung, W. L. Roberts, M. A. Oehlschlaeger, C.-J. Sung, A. Farooq, Compositional effects on the ignition of FACE gasolines, *Combustion and Flame* 169 (2016) 171–193. doi:10.1016/j.combustflame.2016.04.010.
- [21] E. Hairer, G. Wanner, *Solving Ordinary Differential Equations II*, Springer Berlin Heidelberg, Berlin, Heidelberg, 1996. doi:10.1007/978-3-642-05221-7.
- [22] M. J. McNenly, R. A. Whitesides, D. L. Flowers, Faster solvers for large kinetic mechanisms using adaptive preconditioners, *Proceedings of the Combustion Institute* 35 (1) (2015) 581–587. doi:10.1016/j.proci.2014.05.113.

- [23] F. Perini, E. Galligani, R. D. Reitz, An Analytical Jacobian Approach to Sparse Reaction Kinetics for Computationally Efficient Combustion Modeling with Large Reaction Mechanisms, *Energy & Fuels* 26 (8) (2012) 4804–4822. doi:10.1021/ef300747n.
- [24] D. A. Schwer, J. E. Tolsma, W. H. Green, P. I. Barton, On upgrading the numerics in combustion chemistry codes, *Combustion and Flame* 128 (3) (2002) 270–291. doi:10.1016/S0010-2180(01)00352-2.
- [25] C. Safta, H. N. Najm, O. Knio, TChem - A Software Toolkit for the Analysis of Complex Kinetic Models (2011) 56doi:10.2172/1113874.
- [26] K. E. Niemeyer, N. J. Curtis, C. J. Sung, pyJac: Analytical Jacobian generator for chemical kinetics, *Computer Physics Communications* 215 (2017) 188–203. doi:10.1016/j.cpc.2017.02.004.
- [27] L. Antonelli, P. D’Ambra, Dynamic Load Balancing for High-Performance Simulations of Combustion in Engine Applications, in: 2011 19th International Euromicro Conference on Parallel, Distributed and Network-Based Processing, IEEE, 2011, pp. 133–140. doi:10.1109/PDP.2011.88.
- [28] Y. Shi, W. H. Green, H. W. Wong, O. O. Oluwole, Accelerating multi-dimensional combustion simulations using GPU and hybrid explicit/implicit ODE integration, *Combustion and Flame* 159 (7) (2012) 2388–2397. doi:10.1016/j.combustflame.2012.02.016.
- [29] J. Kodavasal, K. Harms, P. Srivastava, S. Som, S. Quan, K. Richards, M. García, Development of a Stiffness-Based Chemistry Load Balanc-

- ing Scheme, and Optimization of Input/Output and Communication, to Enable Massively Parallel High-Fidelity Internal Combustion Engine Simulations, *Journal of Energy Resources Technology* 138 (5) (sep 2016). doi:10.1115/1.4032623.
- [30] T. Zirwes, F. Zhang, P. Habisreuther, J. A. Denev, H. Bockhorn, D. Trimis, *Optimizing Load Balancing of Reacting Flow Solvers in OpenFOAM for High Performance Computing* (2018).
- [31] J. Muela, R. Borrell, J. Ventosa-Molina, L. Jofre, O. Lehmkuhl, C. D. Pérez-Segarra, A dynamic load balancing method for the evaluation of chemical reaction rates in parallel combustion simulations, *Computers and Fluids* 190 (2019) 308–321. doi:10.1016/j.compfluid.2019.06.018.
- [32] E. Anderson, Z. Bai, C. Bischof, S. Blackford, J. Demmel, J. Dongarra, J. D. Croz, A. Greenbaum, S. Hammerling, A. McKenney, D. Sorensen, *LAPACK Users' Guide: Third Edition*, 3rd Edition, Society for Industrial and Applied Mathematics, 1999.
- [33] H. Kahila, O. Kaario, Z. Ahmad, M. Ghaderi Masouleh, B. Tekgül, M. Larmi, V. Vuorinen, A large-eddy simulation study on the influence of diesel pilot spray quantity on methane-air flame initiation, *Combustion and Flame* 206 (2019) 506–521. doi:10.1016/j.combustflame.2019.05.025.
- [34] H. Kahila, *Numerical modeling of spray-assisted dual-fuel ignition*, Ph.D. thesis, Aalto University (2019).

- [35] A. Imren, D. Haworth, On the merits of extrapolation-based stiff ODE solvers for combustion CFD, *Combustion and Flame* 174 (dec 2016). doi:10.1016/j.combustflame.2016.09.018.
- [36] OpenFOAM v6 release notes, <https://openfoam.org/release/6/>, accessed: 2021-02-18.
- [37] G. P. Smith, D. M. Golden, M. Frenklach, N. W. Moriarty, B. Eite-
neer, M. Goldenberg, C. T. Bowman, R. K. Hanson, S. Song, W. C. G.
Jr., V. V. Lissianski, Z. Qin, GRI-Mech 3.0, [http://combustion.
berkeley.edu/gri-mech/](http://combustion.berkeley.edu/gri-mech/) (1999).
- [38] T. Yao, Y. Pei, B. J. Zhong, S. Som, T. Lu, K. H. Luo, A com-
pact skeletal mechanism for n-dodecane with optimized semi-global low-
temperature chemistry for diesel engine simulations, *Fuel* 191 (2017)
339–349. doi:10.1016/j.fuel.2016.11.083.
- [39] A. Kazakov, M. Frenklach, Reduced Reaction Sets based on GRI-
Mech 1.2, <http://combustion.berkeley.edu/drm/>, accessed: 2021-
10-21 (2005).
- [40] R. Issa, B. Ahmadi-Befrui, K. Beshay, A. Gosman, Solution of the im-
plicitly discretised reacting flow equations by operator-splitting, *Journal of Computational Physics* 93 (2) (1991) 388–410. doi:10.1016/
0021-9991(91)90191-m.
- [41] I. Morev, M. Gadalla, S. Karimkashi, J. Kannan, A. Sha-
hanaghi, B. Tekgöl, O. Kaario, V. Vuorinen, GitHub Repository:

- DLBFoam-Advanced-Tutorials, <https://github.com/Aalto-CFD/DLBFoam-Advanced-Tutorials> (2021).
- [42] Mahti supercomputer specifications, <https://docs.csc.fi/computing/systems-mahti/>, accessed: 2021-10-21.
- [43] H. Kahila, A. Wehrfritz, O. Kaario, V. Vuorinen, Large-eddy simulation of dual-fuel ignition: Diesel spray injection into a lean methane-air mixture, *Combustion and Flame* 199 (2019) 131–151. doi:10.1016/j.combustflame.2018.10.014.
- [44] B. Tekgül, H. Kahila, O. Kaario, V. Vuorinen, Large-eddy simulation of dual-fuel spray ignition at different ambient temperatures, *Combustion and Flame* 215 (2020) 51–65. doi:10.1016/j.combustflame.2020.01.017.
- [45] B. Tekgül, H. Kahila, S. Karimkashi, O. Kaario, Z. Ahmad, É. Lendormy, J. Hyvönen, V. Vuorinen, Large-eddy simulation of spray assisted dual-fuel ignition under reactivity-controlled dynamic conditions, *Fuel* 293 (2021) 120295. doi:10.1016/j.fuel.2021.120295.
- [46] J. Kannan, M. Gadalla, B. Tekgül, S. Karimkashi, O. Kaario, V. Vuorinen, Large eddy simulation of diesel spray assisted dual-fuel ignition: A comparative study on two n-dodecane mechanisms at different ambient temperatures, *International Journal of Engine Research* (2020) 1–12doi:10.1177/1468087420946551.
- [47] J. Kannan, M. Gadalla, B. Tekgül, S. Karimkashi, O. Kaario, V. Vuorinen, Large-eddy simulation of tri-fuel ignition: diesel spray-assisted igni-

- tion of lean hydrogen–methane–air mixtures, *Combustion Theory and Modelling* (2021) 1–24. doi:10.1080/13647830.2021.1887525.
- [48] S. Karimkashi, H. Kahila, O. Kaario, M. Larmi, V. Vuorinen, A numerical study on combustion mode characterization for locally stratified dual-fuel mixtures, *Combustion and Flame* 214 (2020) 121–135. doi:10.1016/j.combustflame.2019.12.030.
- [49] S. Karimkashi, H. Kahila, O. Kaario, M. Larmi, V. Vuorinen, Numerical study on tri-fuel combustion: Ignition properties of hydrogen-enriched methane-diesel and methanol-diesel mixtures, *International Journal of Hydrogen Energy* 45 (7) (2020) 4946–4962. doi:10.1016/j.ijhydene.2019.12.033.
- [50] M. Gadalla, J. Kannan, B. Tekgül, S. Karimkashi, O. Kaario, V. Vuorinen, Large-eddy simulation of tri-fuel combustion: Diesel spray assisted ignition of methanol-hydrogen blends, *International Journal of Hydrogen Energy* (May 2021). doi:10.1016/j.ijhydene.2021.03.238.
- [51] M. Gadalla, J. Kannan, B. Tekgül, S. Karimkashi, O. Kaario, V. Vuorinen, Large-Eddy Simulation of ECN Spray A: Sensitivity Study on Modeling Assumptions, *Energies* 13 (13) (2020) 3360. doi:10.3390/en13133360.
- [52] S. A. Skeen, J. Manin, L. M. Pickett, Simultaneous formaldehyde PLIF and high-speed schlieren imaging for ignition visualization in high-pressure spray flames, *Proceedings of the Combustion Institute* 35 (3) (2015) 3167–3174. doi:10.1016/j.proci.2014.06.040.

- [53] R. S. Barlow, J. H. Frank, Effects of turbulence on species mass fractions in methane/air jet flames, in: Symposium (International) on Combustion, Vol. 27, 1998, pp. 1087–1095. doi:10.1016/S0082-0784(98)80510-9.
- [54] H. Pitsch, H. Steiner, Large-eddy simulation of a turbulent piloted methane/air diffusion flame (Sandia flame D), *Physics of Fluids* 12 (10) (2000) 2541–2554. doi:10.1063/1.1288493.
- [55] A. W. Vreman, B. A. Albrecht, J. A. van Oijen, L. P. de Goey, R. J. Bastiaans, Premixed and nonpremixed generated manifolds in large-eddy simulation of Sandia flame D and F, *Combustion and Flame* 153 (3) (2008) 394–416. doi:10.1016/j.combustflame.2008.01.009.
- [56] A. Bertels, B. Kober, A. Rittler, A. Kempf, Large-Eddy Simulation of Sandia Flame D with Efficient Explicit Filtering, *Flow, Turbulence and Combustion* 102 (4) (2019) 887–907. doi:10.1007/s10494-018-9997-0.
- [57] A. Garmory, E. Mastorakos, Sensitivity analysis of LES-CMC predictions of piloted jet flames, *International Journal of Heat and Fluid Flow* 39 (2013) 53–63. doi:10.1016/j.ijheatfluidflow.2012.11.007.
- [58] D. A. Lysenko, I. S. Ertesvåg, K. E. Rian, Numerical simulations of the Sandia Flame D using the eddy dissipation concept, *Flow, Turbulence and Combustion* 93 (4) (2014) 665–687. doi:10.1007/s10494-014-9561-5.

- [59] B. Tekgül, P. Peltonen, H. Kahila, I. Morev, M. Gadalla, GitHub Repository: DLBFoam, <https://github.com/Aalto-CFD/DLBFoam> (2021).